

GROUP DELAY DESCRIPTION FOR BROADBAND PULSES

M. Ware*, S. A. Glasgow†, and J. Peatross†

1. INTRODUCTION

The traditional concept of group delay usually arises in connection with an expansion of the phase delay for an electromagnetic pulse. In this context, the group delay function (evaluated at a single ‘carrier’ frequency) describes the time required for a pulse to traverse a given displacement. However, if the bandwidth of the pulse encompasses a substantial portion of a resonance structure the expansion fails to converge over the relevant range of frequencies. Because of this failure, traditional group delay suffers severe shortcomings when applied to broadband pulse propagation.^{1–4} We recently introduced a method for describing pulse delay^{5,6} in which the group delay function naturally arises. In contrast to the traditional formulation of group delay, this method retains validity for pulses of arbitrary bandwidth propagating in linear dielectrics (including cases where the spectrum overlaps resonances in the medium). In this work we give an overview of this method of description and demonstrate how it may be applied to gain insight into the behavior of broadband electromagnetic pulses. As an illustration we show how the method may be applied to the well-known precursor problem, where the traditional formulation of group delay fails.

2. PULSE DELAY TIME

To concretely discuss delay times, we first define the arrival time of a pulse at a point. Arrival times defined in terms of the advent of some pulse feature (such as the peak) at a point can be ambiguous, since the pulse shape can change dramatically during propagation (e.g., in a precursor field a pulse may evolve two peaks). In the

*National Institute of Standards and Technology, Gaithersburg MD.

†Brigham Young University, Provo UT.

present formulation we avoid this ambiguity by defining the arrival time as a time expectation⁷ of the electromagnetic flux:

$$\langle t \rangle_{\mathbf{r}} \equiv \int_{-\infty}^{\infty} t \rho(\mathbf{r}, t) dt \quad (1)$$

where $\rho(\mathbf{r}, t)$ is a normalized temporal distribution of the Poynting flux at \mathbf{r} :

$$\rho(\mathbf{r}, t) \equiv \hat{\eta} \cdot \mathbf{S}(\mathbf{r}, t) \Big/ \hat{\eta} \cdot \int_{-\infty}^{\infty} \mathbf{S}(\mathbf{r}, t) dt \quad (2)$$

The Poynting vector is defined as usual:

$$\mathbf{S}(\mathbf{r}, t) \equiv \mathbf{E}(\mathbf{r}, t) \times \frac{\mathbf{B}(\mathbf{r}, t)}{\mu_0} \quad (3)$$

We assume that the propagation medium is neutral, nonconducting, and nonmagnetic. The unit vector $\hat{\eta}$ defines the direction in which the energy flow is detected. It plays a role in angularly dispersive systems,⁸ but is unimportant in this work since we consider propagation in only one dimension.

Using this definition for arrival time, the delay Δt between the time when a pulse arrives at a point \mathbf{r}_0 and when it arrives at a point $\mathbf{r} \equiv \mathbf{r}_0 + \Delta \mathbf{r}$ is found naturally from

$$\Delta t \equiv \langle t \rangle_{\mathbf{r}} - \langle t \rangle_{\mathbf{r}_0} \quad (4)$$

After transforming Eq. (4) into the frequency domain and inserting the frequency solution to Maxwell's equations, we can write the delay time as the sum of two terms with intuitive interpretations:

$$\Delta t = \Delta t_G(\mathbf{r}) + \Delta t_R(\mathbf{r}_0) \quad (5)$$

For details on how this expression is obtained, see Refs. [5] and [6].

The first term in Eq. (5), the *net group delay*, is a spectral average of the group delay function weighted by the spectral intensity that is experienced at the final point \mathbf{r} :

$$\Delta t_G(\mathbf{r}) \equiv \int_{-\infty}^{\infty} \left(\frac{\partial \text{Re} \mathbf{k}}{\partial \omega} \cdot \Delta \mathbf{r} \right) \rho(\mathbf{r}, \omega) d\omega \quad (6)$$

where $\rho(\mathbf{r}, \omega)$ is given by

$$\rho(\mathbf{r}, \omega) \equiv \hat{\eta} \cdot \mathbf{S}(\mathbf{r}, \omega) \Big/ \hat{\eta} \cdot \int_{-\infty}^{\infty} \mathbf{S}(\mathbf{r}, \omega) d\omega \quad (7)$$

The frequency representation of the Poynting vector, $\mathbf{S}(\mathbf{r}, \omega)$, is found from the Fourier transforms of the electric and magnetic fields in the usual manner. The

distribution $\rho(\mathbf{r}, \omega)$ is a spectral density function (i.e., it has units of $1/\omega$) which describes the fraction of the pulse's flux that may be associated with a given frequency range. Note that the distribution $\rho(\mathbf{r}, \omega)$ is evaluated at the *final* point, so that only the spectral components that actually arrive at \mathbf{r} contribute to the delay.

Equation (6) explicitly demonstrates the connection between the delay time for a pulse and the group delay function. Note the close resemblance between Eq. (1) and Eq. (6). Both are expectation integrals, the former being executed as a 'center-of-mass' integral in time, the later being executed in the frequency domain on the group delay function, $\partial \text{Re } \mathbf{k} / \partial \omega \cdot \Delta \mathbf{r}$. In contrast to the traditional group delay, in Eq. (6) the group delay function evaluated at every frequency present in the final pulse influences the delay time as recorded by the time 'center-of-mass'.

The second term in Eq. (5) arises from a reshaping of the spectrum through absorption (or amplification). It is given by

$$\Delta t_R(\mathbf{r}_0) \equiv T [e^{-\text{Im } \mathbf{k} \cdot \Delta \mathbf{r}} \mathbf{E}(\mathbf{r}_0, \omega)] - T[\mathbf{E}(\mathbf{r}_0, \omega)] \quad (8)$$

where T is the arrival time given in Eq. (1), but written as a function of the pulse spectrum rather than its temporal profile:

$$\langle t \rangle_{\mathbf{r}} = T[\mathbf{E}(\mathbf{r}, \omega)] \quad (9)$$

where

$$T[\mathbf{E}(\mathbf{r}, \omega)] \equiv -i \frac{\hat{\eta} \cdot \int_{-\infty}^{\infty} \frac{\partial \mathbf{E}(\mathbf{r}, \omega)}{\partial \omega} \times \frac{\mathbf{B}^*(\mathbf{r}, \omega)}{\mu_0} d\omega}{\hat{\eta} \cdot \int_{-\infty}^{\infty} \mathbf{S}(\mathbf{r}, \omega) d\omega} \quad (10)$$

In Eq. (10), the function T depends only on the electric field since the magnetic field can be written in terms of the electric field using the complex index of refraction for the propagation medium.

The reshaping delay Δt_R is evaluated at \mathbf{r}_0 , *before* propagation takes place. It is the difference between the pulse arrival time at \mathbf{r}_0 *without* and *with* the spectral amplitude that will be lost (in the absorbing case) during propagation. Since Δt_R uses the phase of the fields in the initial pulse, the reshaping delay is sensitive to how the pulse is organized. It measures the effect of absorption on a pulse and is sensitive to the pulse's state of chirp. If the pulse experiences roughly the same attenuation or amplification over its entire spectrum (as is the case for a pulse far from resonance or a sufficiently narrowband pulse near a resonance) the reshaping delay is minimal.

Equation (5) gives the delay between the 'center-of-mass' arrival times for any two points in a medium regardless of how the pulse evolves during transit. Since the form is obtained without approximation, it is valid for pulses with arbitrary bandwidths and for arbitrary propagation distances. This formalism does not attempt to define a specific 'group velocity' as being representative of the overall pulse propagation. Rather we have demonstrated that the delay between arrival times at two points is related to a linear superposition of group delays weighted by the

pulse's spectral content, as in Eq. (6). By taking the limit of small separation a local velocity can be defined at each point along the propagation.⁷ However, we prefer to consider the difference in arrival times at two discretely separated points since this is more directly applicable to experiment.

The formulation presented here can be thought of as a generalization of the traditional concept of group delay, and in the narrowband limit the delay time given by Eq. (5) reduces to the traditional expression derived using expansion techniques. In this limit the reshaping delay tends to zero, and the normalized spectral distribution approaches a delta function $\rho(\mathbf{r}, \omega) \rightarrow \delta(\omega - \bar{\omega})$ where $\bar{\omega}$ is the central frequency of the pulse. The total delay is then calculated from Eq. (6) as $\Delta t = \partial \text{Re } \mathbf{k} / \partial \omega|_{\bar{\omega}} \cdot \Delta \mathbf{r}$, in agreement with the well verified observation⁹⁻¹³ that a pulse travels at the group velocity evaluated at $\bar{\omega}$ in the narrowband limit. It is important to note that group delay (in both broadband and narrowband cases) measures the delay between when pulse energy is *observed* at two points, and not necessarily the velocity at which pulse energy is *transported* from one point to the other. When a pulse is absorbed or amplified in the propagation medium, this delay does not necessarily indicate energy transport or information transfer since the propagation medium exchanges energy asymmetrically with the leading and trailing portions of a pulse.¹⁴⁻¹⁶

3. APPLICATION TO A BROADBAND PULSE

To illustrate the use of the formulation introduced above we consider a specific example of a broadband pulse whose spectrum is centered near a resonance in the medium. For this example we employ the Lorentz model with a single resonance frequency ω_0 and a damping frequency γ (please note, however, that the formulation presented above is independent of model). The complex index of refraction in this model is given by

$$[n(\omega)]^2 = 1 + \frac{f\omega_p^2}{\omega_0^2 - \omega^2 - i\gamma\omega}, \quad (11)$$

where ω_p is the plasma frequency and f is the oscillator strength. We choose the medium parameters as $\omega_0 = 50\gamma/7$, $\omega_p = 25\sqrt{5}\gamma/7$, and $f = 1$. (The parameters in this example closely correspond to those in Ref. [17].) The group delay function for these parameters is plotted in Fig. 1(a). If we ignore the frequencies near ω_0 (which will be absorbed after propagating a significant distance), Fig. 1(a) shows that low frequency spectral components have slightly longer delay times than high frequency components. This indicates that in the mature dispersion regime (i.e. when $\Delta \mathbf{r}$ is large) a pulse will be chirped such that high frequency components arrive at a point before low frequency components.

We consider a pulse with a Gaussian electric field at \mathbf{r}_0 , given by

$$\mathbf{E}(\mathbf{r}_0, t) = \mathbf{E}_0 \exp(-t^2/\tau^2) \cos(\bar{\omega}t) \quad (12)$$

as it propagates through this medium. The pulse parameters are chosen as $\tau = 0.5/\gamma$ and $\bar{\omega} = 10\gamma$. This results in a pulse whose spectrum is broad compared to the resonance, and is centered slightly above ω_0 . In this situation the traditional expansion method for group delay fails, since it predicts the delay time based on

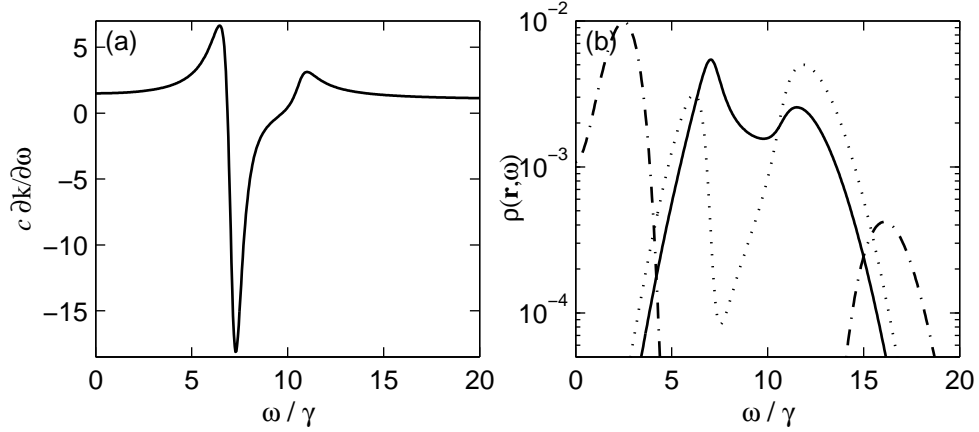


Figure 1. (a) Group delay function normalized by $\Delta r/c$. (b) Normalized spectral distribution for propagation distances of 8.2×10^{-3} (solid), 0.82 (dotted), and 82 (dash-dot) absorption depths.

the group delay function evaluated at the central frequency in the *initial* pulse. However, in this example the energy associated with spectral components near $\bar{\omega}$ is quickly absorbed as the pulse propagates, so these spectral components do not influence the arrival at observation point located at points deeper in the medium. This shows why the prediction of propagation delay needs to be made using the spectrum that will survive propagation, as is done in Eq. (6).

Equation (5) can be used to predict the delay time for this pulse. Figure 1(b) shows the normalized spectral distribution $\rho(\mathbf{r}, \omega)$ for three values of $\Delta \mathbf{r}$. The relative net group delay ($c\Delta t_G/\Delta r$) calculated using (6) is plotted in Fig. 2(a) as a function of the propagation depth. (The points at which the spectral distributions in Fig. 1(b) occur are marked with stars.) For small displacements, Δt_G is negative since the near-resonance components of the pulse spectrum still affect the expectation in Eq. (6). As the pulse propagates further into the medium and experiences absorption, the longer delay times of the off-resonance components dominate the expectation resulting in the eventual subluminal delay times generally observed for broadband pulses.

Even though the initial electric field in Eq. (12) is symmetric, the Poynting flux at \mathbf{r}_0 has a significant chirp. (This occurs because of the connection required by Maxwell's equations between \mathbf{E} and \mathbf{B} in a dielectric medium.) Thus, the reshaping delay has a noticeable effect on the total delay time at very shallow propagation depths (note the log scale on the propagation distance). At about one absorption depth the reshaping delay approaches a constant value, and the relative reshaping delay, $c\Delta t_R/\Delta r$, (plotted in Fig. 2(a)) goes quickly to zero as the propagation distance increases beyond this depth. At large propagation depths the total delay is dominated by the net group delay.

The total delay is given by the sum of the reshaping and net group delays as in Eq. (5). The relative total delay, $c\Delta t/\Delta r$, is plotted in Fig. 2(a). In the mature

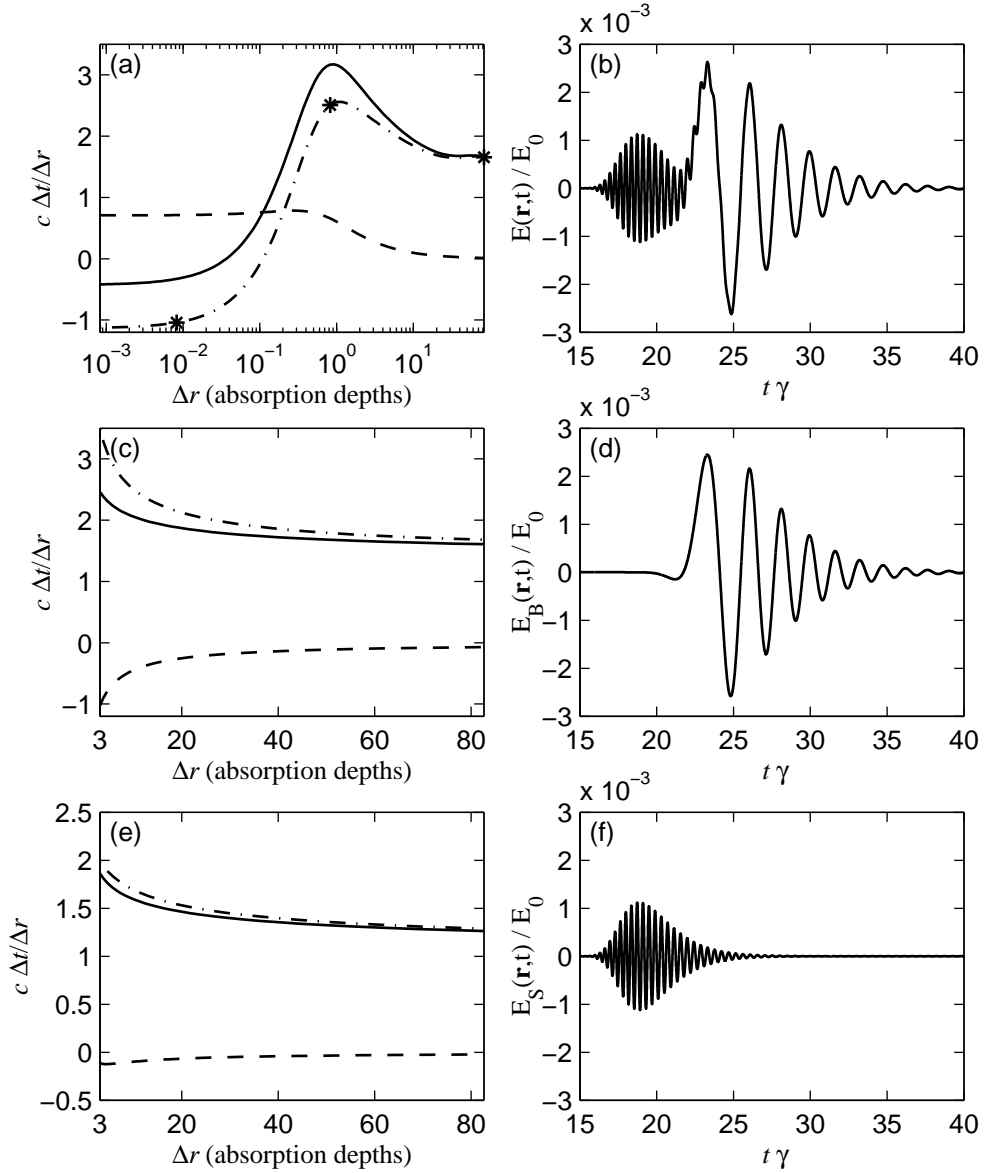


Figure 2. (a) Relative net group delay (dash-dot), reshaping delay (dash), and total delay (solid) as a function of propagation depth for the entire pulse. The stars indicate the absorption depths at which the distributions in Fig. 1(b) are evaluated. (b) Temporal profile of the pulse after propagating 82 absorption depths. (c) Relative net group delay (dash-dot), reshaping delay (dash), and total delay (solid) as a function of propagation depth for the low frequency component. (d) Temporal profile of the low frequency component after propagating 82 absorption depths. Figures (e)–(f) repeat (c)–(d) for the high frequency component.

dispersion regime the delay times settle into a stable situation where the delay of a pulse is given almost entirely by the net group delay. The reshaping delay plays a minimal role in this regime since absorption is small here (the spectral components that experience significant absorption having already been removed from the pulse). This behavior is easily observed in Fig. 2(a).

4. INDIVIDUAL PRECURSOR FIELDS

Figure 2(b) shows the temporal profile of the electric field for this pulse at 82 absorption depths into the medium. Notice that the high frequency components arrive first as would be predicted from the group delay function. For the pulse/medium parameters that we have used here, there are two distinct bumps in the final pulse. In the traditional asymptotic treatment of pulses in the mature dispersion limit, the high frequency component is referred to as the Sommerfeld precursor and the low frequency component is referred to as the Brillouin precursor. To this point we have considered only the delay of the pulse taken as a whole, so that the total delay is a weighted average of the delay times for the two individual precursor components. It is also interesting to consider the delay time of the two precursor fields separately.

Because the Fourier transform is a linear operation, we can separate the spectrum of a pulse propagating in a single resonance absorber (with resonance frequency ω_0) into two pieces as follows:

$$\mathbf{E}(\mathbf{r}, \omega) = \mathbf{E}_B(\mathbf{r}, \omega) + \mathbf{E}_S(\mathbf{r}, \omega) \quad (13)$$

where

$$\mathbf{E}_B(\mathbf{r}, \omega) = \begin{cases} \mathbf{E}(\mathbf{r}, \omega) & , \quad |\omega| \leq \omega_0 \\ 0 & , \quad |\omega| > \omega_0 \end{cases} \quad (14)$$

$$\mathbf{E}_S(\mathbf{r}, \omega) = \begin{cases} 0 & , \quad |\omega| \leq \omega_0 \\ \mathbf{E}(\mathbf{r}, \omega) & , \quad |\omega| > \omega_0 \end{cases} \quad (15)$$

The temporal profile of the pulse is then given by

$$\mathbf{E}(\mathbf{r}, t) = \mathbf{E}_S(\mathbf{r}, t) + \mathbf{E}_B(\mathbf{r}, t) \quad (16)$$

where the two terms in Eq. (16) are the inverse Fourier transforms of Eqs. (14) and (15). The term $\mathbf{E}_S(\mathbf{r}, t)$ is then the ‘above resonance’ portion of the pulse, and $\mathbf{E}_B(\mathbf{r}, t)$ is the ‘below resonance’ portion.

If a pulse’s initial spectrum $\mathbf{E}(\mathbf{r}_0, \omega)$ has significant on-resonance amplitude, then $\mathbf{E}_S(\mathbf{r}_0, \omega)$ and $\mathbf{E}_B(\mathbf{r}_0, \omega)$ will have a significant discontinuity at ω_0 . Because an abrupt discontinuity in frequency requires a broad temporal profile, $\mathbf{E}_S(\mathbf{r}_0, t)$ and $\mathbf{E}_B(\mathbf{r}_0, t)$ will be poorly localized. In this case the two terms have little significance individually except that when added together they produce the temporal profile of the total field. However, as the pulse propagates the on-resonance amplitude of $\mathbf{E}(\mathbf{r}, \omega)$ decreases and the discontinuity becomes less important. Eventually the discontinuity becomes insignificant, and $\mathbf{E}_S(\mathbf{r}, t)$ and $\mathbf{E}_B(\mathbf{r}, t)$ represent two

independent pulses. The delay times for these two pulses can be tracked separately using Eq. (5).

Figure 2(c) plots the relative delay times for the low frequency component \mathbf{E}_B of the pulse considered in the preceding section. For this plot we place \mathbf{r}_0 (used to calculate Δt_R) three absorption depths beyond the point where the electric field is Gaussian so that the near-resonance portion of the pulse has been significantly attenuated. Figure 2(d) shows the temporal profile of the low frequency component at the same distance as Fig. 2(b). Figures 2(e)–(f) repeat these plots for the high frequency component \mathbf{E}_S . As with the total field, when propagation distance becomes large the reshaping delay becomes negligible and the total delay is given by the net group delay. At these large propagation distances the normalized spectral distribution for the low frequency component \mathbf{E}_B becomes more tightly concentrated about $\omega = 0$ since frequency components near resonance experience the most absorption. Thus the delay time for \mathbf{E}_B approaches the group delay at $\omega = 0$ in the limit of large propagation distance. The spectral distribution for the high frequency component, \mathbf{E}_S , shifts towards higher frequencies at large propagation distances as the near resonance components are absorbed. Thus, the high frequency component approaches an exactly luminal delay in the limit of large propagation distances.

5. CONCLUSION

In this article we have discussed a method for describing pulse delay which is valid for pulses of any bandwidth and showed how it may be applied in a broadband situation where precursor fields are observed. This method correctly describes the delay of a pulse taken in its entirety, and also the delay of the high and low frequency precursor components (i.e., the Sommerfeld and Brillouin precursors) individually. This method does not provide a full description of precursor fields, of course. However, when predicting delay times for a precursor fields, it has some advantages when compared to the asymptotic approach generally employed. The approach used here to study precursor behavior is independent of the model used to describe the medium. In addition, this method is easily generalizable to describe precursor fields in multiple resonance media. (For example, in a two resonance medium there are three precursor fields describing different spectral regions: one below the lower resonance, one above the higher resonance, and one between the two resonances.) Perhaps the most appealing advantage of the approach used here to analyze precursor behavior is its conceptual clarity; we are simply analyzing the behavior of different spectral portions of a pulse after it has propagated a large distance. This notion can sometimes be obscured by the details of the traditional approach.

REFERENCES

1. M. Born and E. Wolf, *Principles of Optics*, sixth ed. (Pergamon, Oxford, 1980).
2. J. D. Jackson, *Classical Electrodynamics*, 3rd ed. (Wiley, New York, 1998).
3. K. E. Oughstun and H. Xiao, Failure of the Quasimonochromatic Approximation for Ultrashort Pulse Propagation in a Dispersive, Attenuative Medium, *Phys. Rev. Lett.* **78**, 642–645 (1997).
4. H. Xiao and K. E. Oughstun, Failure of the group-velocity description for ultrawideband pulse propagation in a causally dispersive, absorptive dielectric, *J. Opt. Soc. Am. B* **16**, 1773–1785 (1999).
5. J. Peatross, S. A. Glasgow, and M. Ware, Average Energy Flow of Optical Pulses in Dispersive Media, *Phys. Rev. Lett.* **84**, 2370–2373 (2000).
6. M. Ware, S. A. Glasgow, and J. Peatross, The Role of Group Velocity in Tracking Field Energy in Linear Dielectrics, *Opt. Express* (2001).
7. R. L. Smith, The Velocities of Light, *Am. J. Phys.* **38**, 978–984 (1970).
8. M. Ware, W. E. Dibble, S. A. Glasgow, and J. Peatross, Energy Flow in Angularly Dispersive Optical Systems, *J. Opt. Soc. Am. B* **18**, 839–845 (2001).
9. R. Y. Chiao, Superluminal (but causal) propagation of wave packets in transparent media with inverted atomic populations, *Phys. Rev. A* **48**, R34–R37 (1993).
10. R. Y. Chiao and A. M. Steinberg, Tunneling Times and Superluminality, *Progress in Optics* **37**, 347–406 (Emil Wolf ed., Elsevier, Amsterdam, 1997).
11. S. Chu and S. Wong, Linear Pulse Propagation in an Absorbing Medium, *Phys. Rev. Lett.* **48**, 738–741 (1982).
12. E. L. Bolda, J. C. Garrison, and R. Y. Chiao, Optical pulse propagation at negative group velocities due to a nearby gain line, *Phys. Rev. A* **49**, 2938–2947 (1994).
13. C. G. B. Garrett and D. E. McCumber, Propagation of a Gaussian Light Pulse through an Anomalous Dispersion Medium, *Phys. Rev. A* **1**, 305–313 (1970).
14. S. A. Glasgow, M. Ware, and J. Peatross, Poynting’s Theorem and Luminal Energy Transport Velocity in Causal Dielectrics, *Phys. Rev. E* **64**, 046610–1–046610–14 (2001).
15. J. Peatross, M. Ware, and S. A. Glasgow, The Role of the Instantaneous Spectrum in Pulse Propagation in Causal Linear Dielectrics, *J. Opt. Soc. Am. A* **18**, 1719–1725 (2001).
16. M. Ware, S. A. Glasgow, and J. Peatross, Energy Transport in Linear Dielectrics, *Opt. Express*, (2001).
17. K. E. Oughstun and C. M. Balictsis, Gaussian Pulse Propagation in a Dispersive, Absorbing Dielectric, *Phys. Rev. Lett.* **77**, 2210–2213 (1996).
18. K. E. Oughstun and G. C. Sherman, *Electromagnetic Pulse Propagation in Causal Dielectrics* (Springer-Verlag, New York, 1994).